Spatiotemporal Oscillations in Biological Molecules: Histidine-Molybdate Interactions

C. V. Krishnan[*]

Department of Chemistry, Stony Brook University, Stony Brook, NY11794-3400, USA
[*]E-mail: chirakkal.krishnan@stonybrook.edu

Investigation of the cyclic voltammetric behaviour of L-histidine in the absence and presence of sodium molybdate revealed that molybdate enhanced the oxidation of histidine. Reduction of the presumed oxidation product of histidine, 2-oxohistidine, produced cathodic current oscillations. The cathodic and anodic currents and the cathodic current oscillations were much higher in the presence of molybdate. A comparison of the cyclic voltammograms also revealed strong interactions of molybdate with histidine and also the presence of molybdate in the oxidized histidine. The U-V absorption spectra indicated specific interaction between histidine and molybdate. Impedance exhibited negative differential resistance (NDR) and impedance loci in one, two, three or four quadrants depending on the applied potential. In the absence of molybdate, somewhat chaotic impedance oscillations instead of NDR were observed. When the concentrations of histidine-molybdate were increased, the impedance spectra observed in four quadrants became more symmetric. When the ratio of histidine to molybdate was changed from 2:1 to 1:1, the NDR observed was better. With increase in pH, a slight cathodic shift was observed in the potential at which NDR was observed. At lower pH, the impedance spectra observed in four quadrants were extended to a wider range of potentials of about 100 mV. At more anodic potentials after the four quadrants impedance spectra, the nature of impedance changed to double capacitance and an inductive loop and then finally to three capacitance curves. In the presence of molybdate, the data suggested that self-assembled layers of histidine-molybdate near the double layer increased the possibility of long range electron transfer. The one electron reduction product of 2-oxohistidine, a free radical, is believed to be responsible for this observed NDR.

1. INTRODUCTION

L-histidine, shown in Figure 1a, is an essential amino acid with an aromatic nitrogen-heterocyclic imidazole side chain. It has $pK_1(\alpha\text{-COOH})$, $pK_2(\alpha\text{-NH}_3^+)$, and $pK_3(\text{imidazole})$ values of 1.78, 8.97 and 5.97 respectively [1]. Its isoelectric point (pH) is 7.47. Relatively high concentrations of

both basic (imidazole) and acidic (imidazolium) forms of the histidine side chain are present in physiological solutions. The neurotransmitter histamine is produced by decarboxylation of histidine**.** Histidine is also an important component of enzymes such as carbonic anhydrase and superoxide dismutase [1]. In carbonic anhydrase, the active form is quickly regenerated by a histidine proton shuttle where the protons are quickly shuttled away from a zinc-bound water molecule [2].

The imidazole side chain makes histidine a common participant in enzyme catalyzed reactions [2]. The nonprotonated imidazole is nucleophilic and can serve as a general base, while the protonated form can serve as a general acid. The charge of histidine changes considerably with small changes in intracellular pH. It serves as an excellent coordinating ligand in metalloproteins. The residue can also serve a role in stabilizing the folded structures of proteins.

All living systems exhibit dynamical spatiotemporal periodicities [3]. Dynamical spatiotemporal oscillations are observed in many electrochemical systems such as anodic metal dissolution, cathodic metal deposition, oxidation of small organic molecules, and reduction of hydrogen peroxide [4-9]. We had reported earlier that the phenomenon of impedance with negative differential resistance and the impedance loci passing through two, three or four quadrants in the complex plane are common in many biological systems [4].
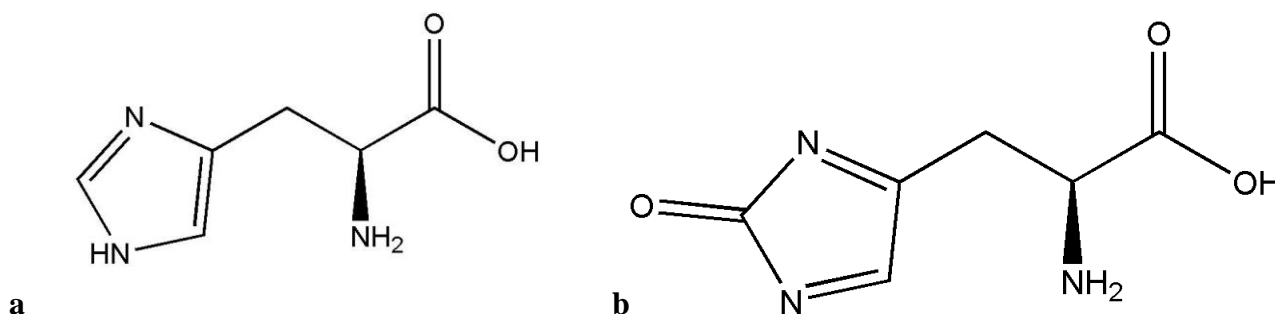
Figure 1. a. Histidine and **b.** 2-Oxohistidine

We had previously observed that two amino acids, lysine and cysteine, exhibited spatiotemporal oscillations by itself and when interacting with DNA and ions such as molybdate [4,10,11]. Our recent admittance measurements of the systems, L-histidine-water and L-histidine-molybdate –water revealed five admittance peaks and a shoulder for histidine and 3 admittance peaks for histidine in the presence of molybdate. These data suggested strong histidine-histidne and histidine-molybdate interactions with water at the double layer [12]. The present investigation compliments the previous one with cyclic voltammetric and impedance measurements.

2. EXPERIMENTAL PART

An EG & G PARC Model 303A SMDE tri-electrode system (mercury working electrode, platinum counter electrode and Ag/AgCl (3.5M KCl) reference electrode) along with Autolab eco chemie was used for cyclic voltammetric and impedance measurements at 298 K. Sodium molybdate

dihydrate and L-histidine were from Sigma. Distilled water was used for preparation of all solutions. J.T. Baker 1.0 N NaOH and 1.0 N HCl were used for pH adjustments. The solutions were purged with N_2 for about 10 minutes before the experiment. Impedance measurements were mostly in the frequency range 1000 Hz to 5 mHz.

3. RESULTS AND DISCUSSION

3.1. Absorption Spectra

The absorption spectra of 0.019 M histidine, 0.0095 M sodium molybdate, and a solution containing 0.019 M histidine and 0.0095 M sodium molybdate are shown in Figure 2.
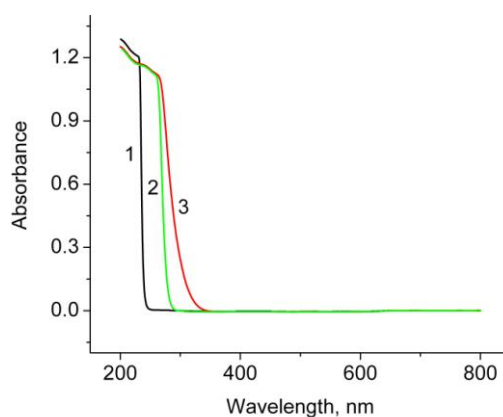
Figure 2. Absorption spectra of 1) 0.019 M histidine, 2) 0.0095 M sodium molybdate, and 3) 0.019 M histidine-0.0095 M sodium molybdate, 1mm cell.

The absorption spectrum observed for the mixture indicated an interaction between histidine and molybdate.

3.2. Cyclic Voltammetry

Cyclic voltammetric measurements in the range 0.0 to -1.0 V and 0.3 to -1.0V at a scan rate of 0.1 V/sec were carried out using 0.19 M histidine. The results shown in Figure 3a, have indicated that the reduction currents are stabilized after the first scan. When the scan range was extended to +0.3V, similar reduction currents were observed for all the three scans (Figure 3b). However, current oscillations were observed. Also there was a slight cathodic shift in the reduction peak, as shown in Figure 3c. There were no well defined oxidation peaks in both scan ranges.

Cyclic voltammetric measurements for a mixture of 0.19 M histidine and 0.095 M sodium molybdate in the scan range 0.0 to -1.0 V and 0.3 to -1.0 V and a scan rate of 0.1V/sec are shown in Figure 4. The results in Figure 4a have indicated the same current irrespective of the number of scans. Also unlike the case of histidine, the presence of molybdate had induced current oscillation at this

range of scan, 0.0 to -1.0 V. When the range of the scan was extended to include a probable slight passivation region of the mercury electrode, similar results were observed as shown in Figure 4b. Also the oxidation peak became well defined. A comparison of the results for the third scan and for the two scan ranges, 0.0 to -1.0 V and 0.3 to -1.0 V, shown in Figure 4c indicated similar results and no shift in potentials for the reduction peaks. Cathodic current oscillations were observed in both cases. These results have indicated that the current oscillations were not arising from any probable passivation of mercury but from the inherent chemistry of the histidine-molybdate mixture.
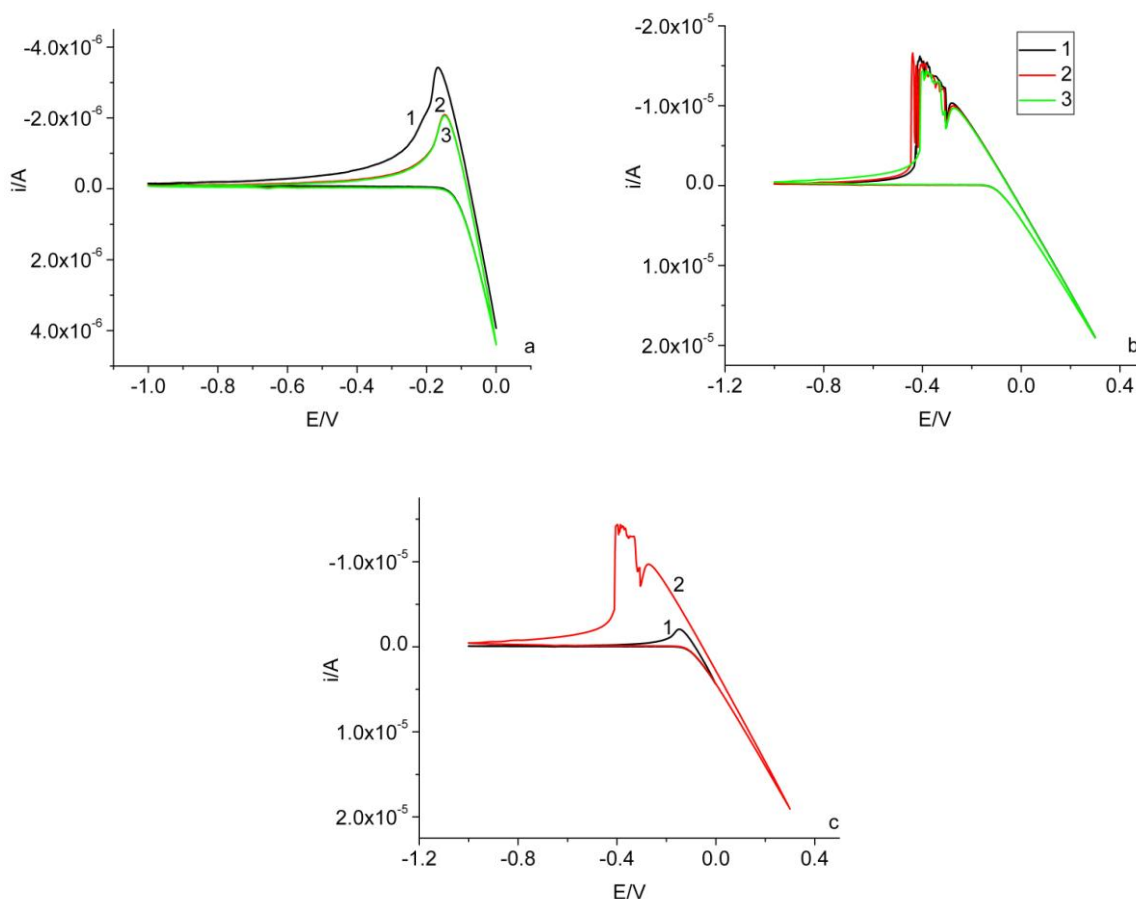
Figure 3. Cyclic voltammograms of 0.19 M histidine, pH 7.4, scan rate 0.1 V/sec, 1) scan 1; 2) scan 2; 3) scan 3; a) 0 to -1.0V; b) 0.3 to -1.0 V; c) 1, 0.0 to -1.0 V, scan 3; 2, 0.3 to -1.0V, scan 3

The results for histidine and histidine-molybdate combination are compared for the third scan in Figure 5a. The data for sodium molybdate are also included. Because of the high cathodic current for the combination of histidine-molybdate, the slight redox activity of histidine was masked in Figure 5a. There was no observable redox activity for molybdate in this potential range. A unique redox behavior with cathodic current oscillations was observed for the mixture containing histidine and molybdate. The results for the mixture with scans in the range +0.3 to -1.0 V at different scan rates are shown in Figure 5b. As expected, both anodic and cathodic currents increased with increasing scan

rate. Cathodic current oscillations were observed in all cases. No background electrolyte was used in these measurements.
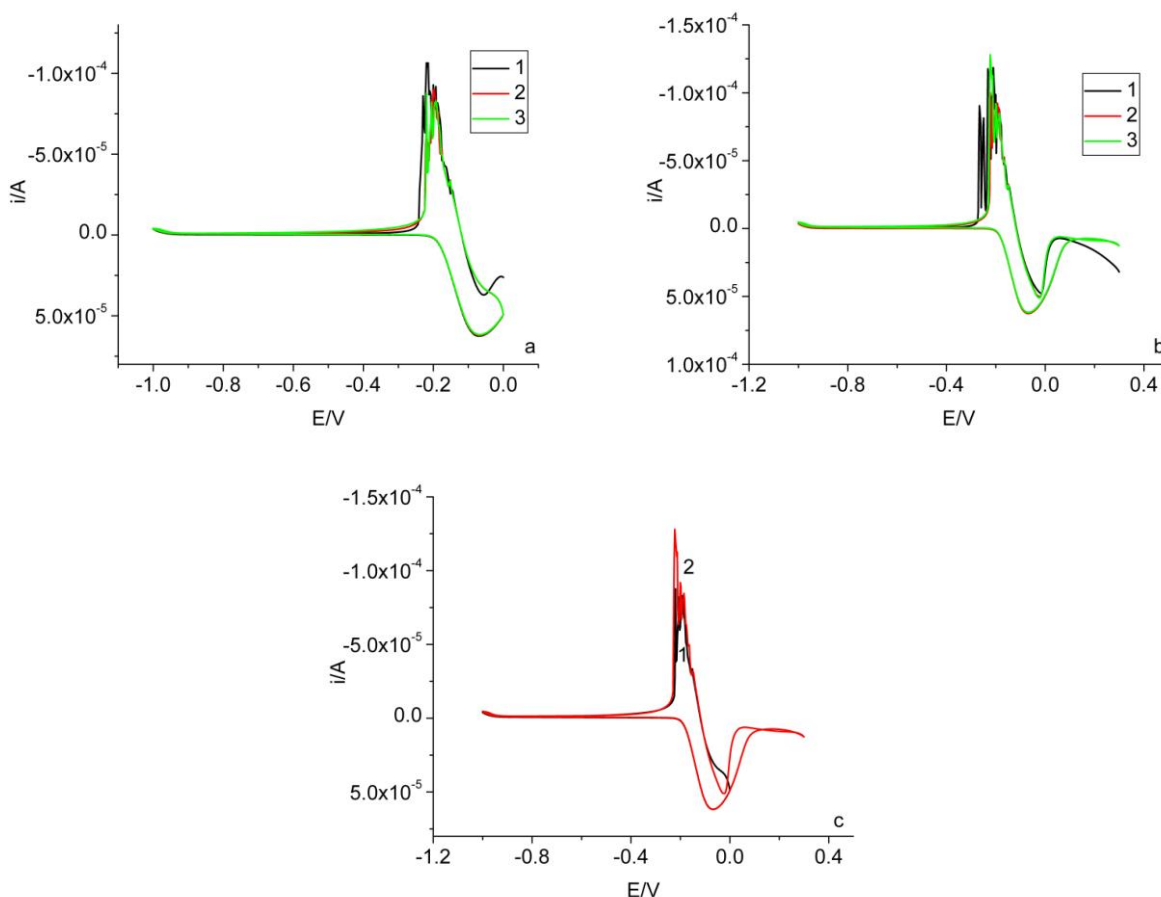
Figure 4. Cyclic voltammograms of 0.19 M histidine - 0.095 M sodium molybdate, pH 8.4, scan rate 0.1 V/sec, 1) scan 1; 2) scan 2; 3) scan 3; a) 0 to -1.0V; b) 0.3 to -1.0 V; c) 1, 0.0 to -1.0 V, scan 3; 2, 0.3 to -1.0V, scan 3
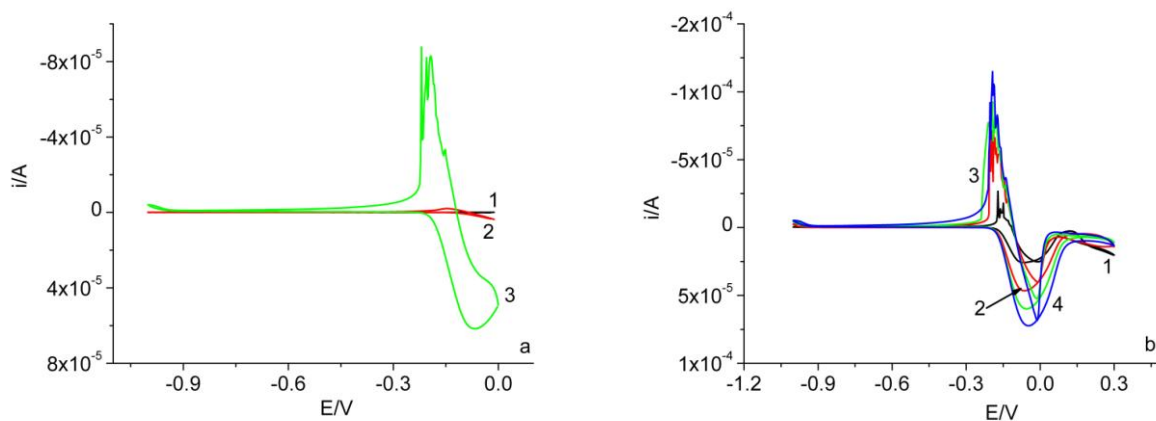
Figure 5. Cyclic voltammograms of a) 1. 0.095 M sodium molybdate, 2. 0.19 M histidine, and 3. a solution containing 0.19 M histidine and 0.095 M sodium molybdate; scan 3, scan rate, 0.1 V/sec; b) a solution containing 0.19 M histidine and 0.095 M sodium molybdate, scan 3, scan rate 1) 0.01, 2) 0.05, 3) 0.1, and 4) 0.15 V/sec

In the absence of any background electrolytes the histidine-sodium molybdate combination will be competing only with water and Na^+ for the surface of mercury at a given applied potential.

A recent study of histidine-histidine dipeptide interactions in the gas phase using density functional theory method with Gaussian 98 program have revealed the presence of six rings. Two of these rings belonged to the imidazole rings of the dipeptide. Four additional rings were from intramolecular hydrogen bonds [2]. Even though we did not use a dipeptide for our measurements, it may be possible to have similar structures at or near the double layer in aqueous solutions and hydrogen bonding with water. This may contribute to the unique admittance spectra we had observed earlier [12]. Also, at negative potentials it is possible to have both the protonated and nonprotonated forms of the histidine to be near the double layer competing with water (dipole).

We had observed earlier that molybdate interacts strongly with other molecules such as cysteine [11]. It is also known that histidine kinase interacts with DNA at the phosphate group [13] and 1-phoshpo and 3-phospho histidines are known. It is possible therefore to have histidine-molybdate interactions at the imidazole nitrogens of histidine in positions 1 and 3. The observed current increase in the presence of molybdate indicated the strong interaction.

Cu,Zn-superoxide dismutase is known to be inactivated by its own reaction product of hydrogen peroxide [14, 15]. It is believed that the histidine residues in the active site of the enzyme are oxidized by H_2O_2. This oxidized histidine was shown to be 2-oxohistidine, shown in Figure 1b [14].

Our cyclic voltammetric results have indicated slight oxidation of histidine. We are attributing this oxidized product to be 2-oxohistidine.

It has been postulated that marking steps in enzyme turnover are due to free radical-mediated oxidative inactivation of enzymes [16]. Metal catalyzed oxidation of enzyme systems make them especially vulnerable to inactivation. Metal-catalyzed oxidation of histidine residues in proteins and human growth hormone are well known [17, 18]. Electrochemical oxidation of histidine and copper-histidine complexes have also been studied in the past using electrodes such as anodic oxidized boron-doped diamond, platinum, gold, vitreous carbon, paraffin-wax impregnated spectroscopic graphite, and glassy carbon [19-23]. Our current results have indicated that there is some oxidation of histidine at the mercury electrode and the oxidation is catalyzed by molybdate.
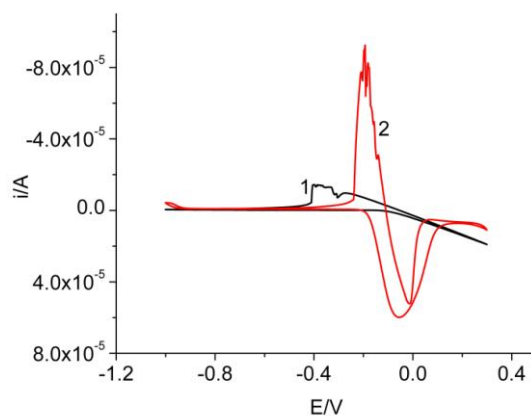
Figure 6. Comparison of cyclic voltammograms of 1) 0.19 M histidine and 2) 0.19 M histidine – 0.095 M sodium molybdate; scan 3, scan rate 0.1 V/sec

A comparison of the cyclic voltammetric data for scan 3 and for the scan range 0.03 to -1.0 V at a scan rate of 0.1 V/sec for 1) 0.19 M histidine and 2) for a mixture of 0.19 M histidine – 0.095 M sodium molybdate mixture are shown in Figure 6. The differences in the potentials for the reduction peaks have indicated that the two oxidized products in the absence and presence of molybdate may be different. We are suggesting that the one with pure histidine is 2-oxohistidine and the one for the mixture may be 2-oxohistidine with attached molybdate by interaction with the imidazole nitrogen. This may account for the observed differences in the cathodic peak positions and the observed higher cathodic current for the histidine-molybdate mixture. A one electron reduction of this product will produce a free radical and may be responsible for the current oscillations, especially in the presence of molybdate.

3.3. Impedance

3.3.1. Impedance spectra of histidine
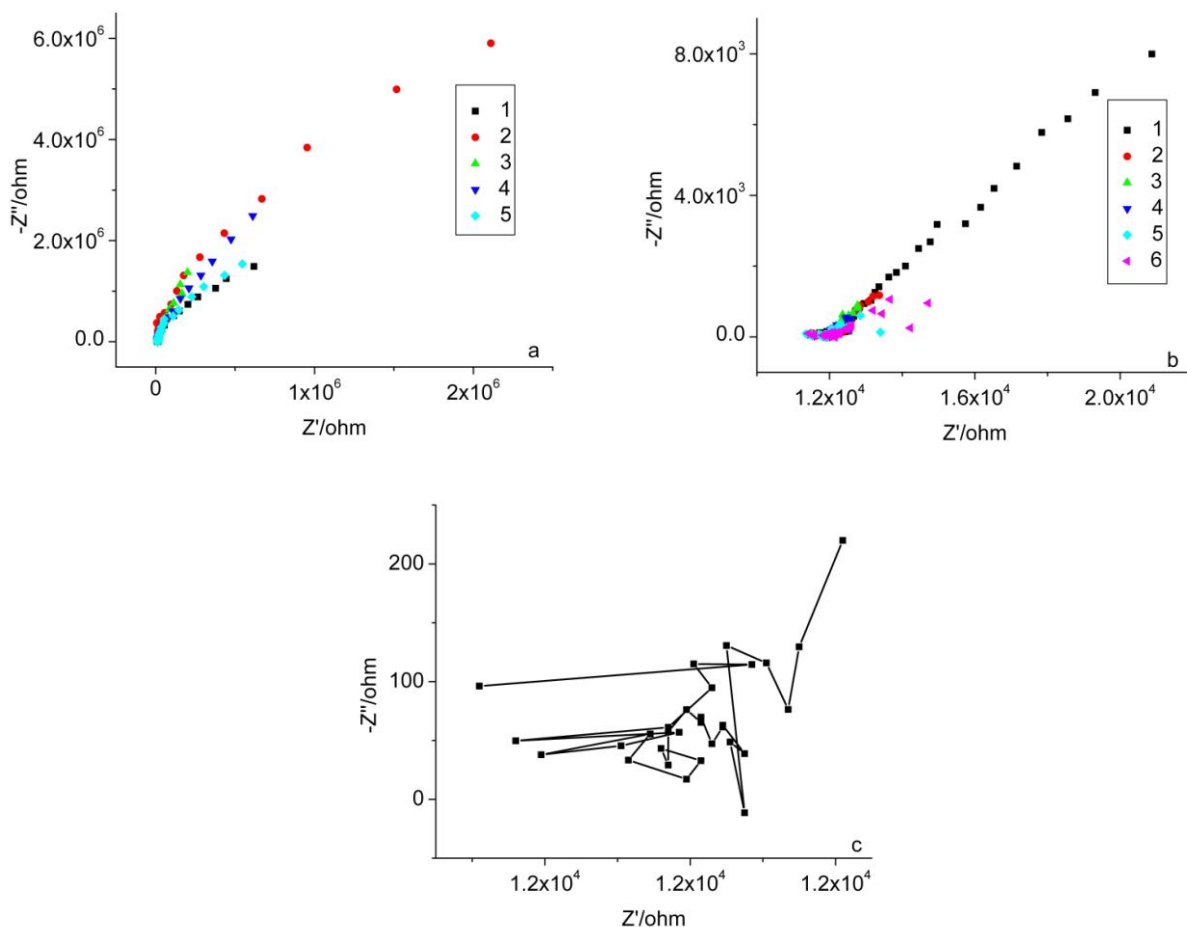
Figure 7. Nyquist plots for 0.19 M histidine at pH 7.4, 1000 Hz to 82 mHz; a) 1) -1.0 V, 2) -0.8 V, 3) -0.6 V, 4) -0.4 V, 5) -0.2 V; b) 1) -0.1 V, 2) -0.05 V, 3) -0.03 V, 4) 0.0 V, 5) 0.05 V, 6) 0.09 V; c) 1000 Hz to 628 mHz, 0.09 V

The Nyquist plots for 0.19 M histidine at pH 7.4 at different potentials are shown in Figure 7. Other than the normal capacitive behavior, nothing unusual was observed in any of these impedance data except at potentials more anodic than 0.0 V. For the sake of clarity and to highlight the scatter with some probable impedance oscillations at high frequencies, the data at 0.09Vwere truncated at 628 mHz (Figure 7c). We have observed more orderly impedance oscillations at high frequencies for cysteine [10]. It must be pointed out that meaningful information on ion/molecule-solvent interactions in the potential range 0.0 to -1.0 V was obtained from admittance [12].

3.3.2. Potential dependence of impedance of 2 to1 histidine to molybdate

We had carried out several impedance measurements using histidine to molybdate in the ratio of 2 to1. The Nyquist plots for 0.19 M histidine-0.095 M sodium molybdate at pH 8.5 and at different potentials are shown in Figure 8. The data shown in Figure 8f at cathodic potentials are for comparison purposes with histidine data. Here again the normal capacitive behavior was observed at cathodic potentials. More interesting features began to appear at anodic potentials starting at 0.0 V. With a gradual anodic shift in potentials, the impedance loci shifted from 1st quadrant to 2nd, 3rd, and 4th quadrants. The frequency at which negative differential resistance occurred varied slightly with the change in potential.
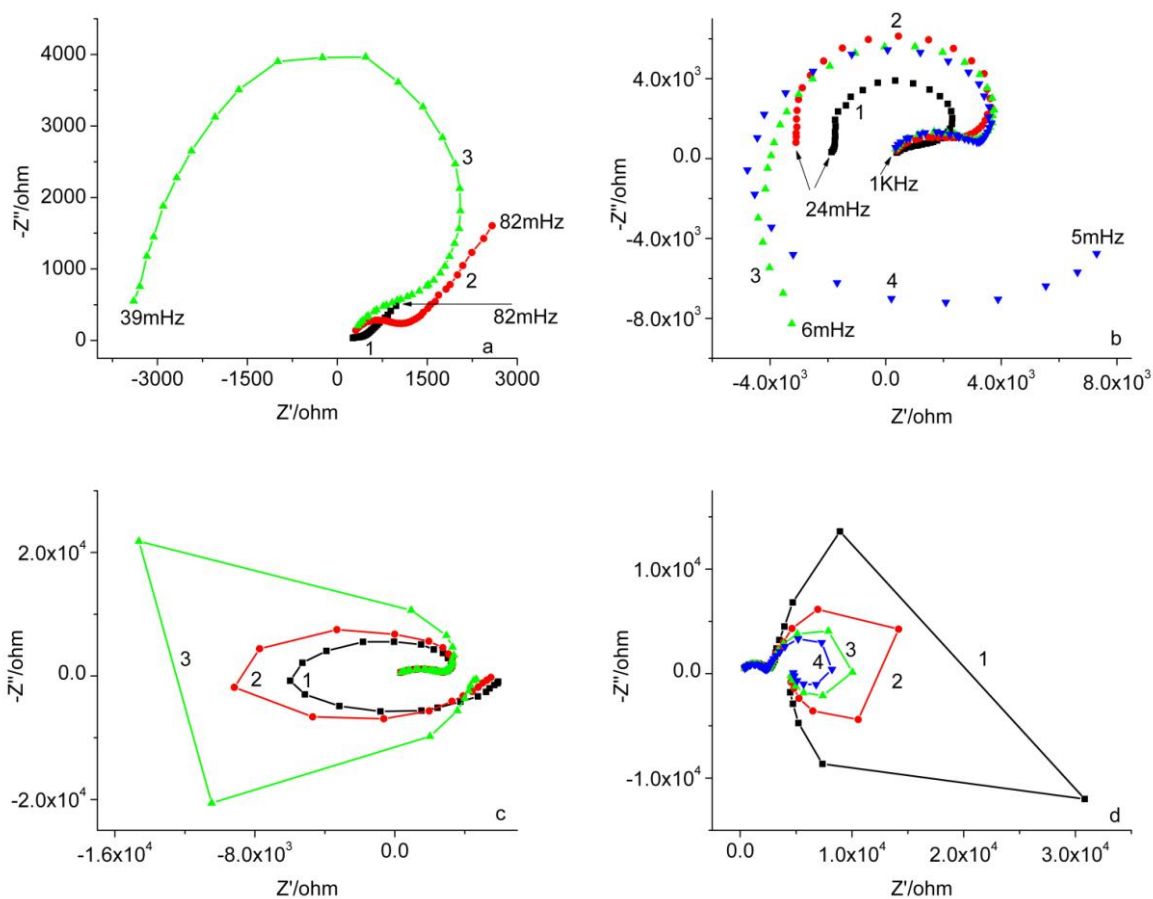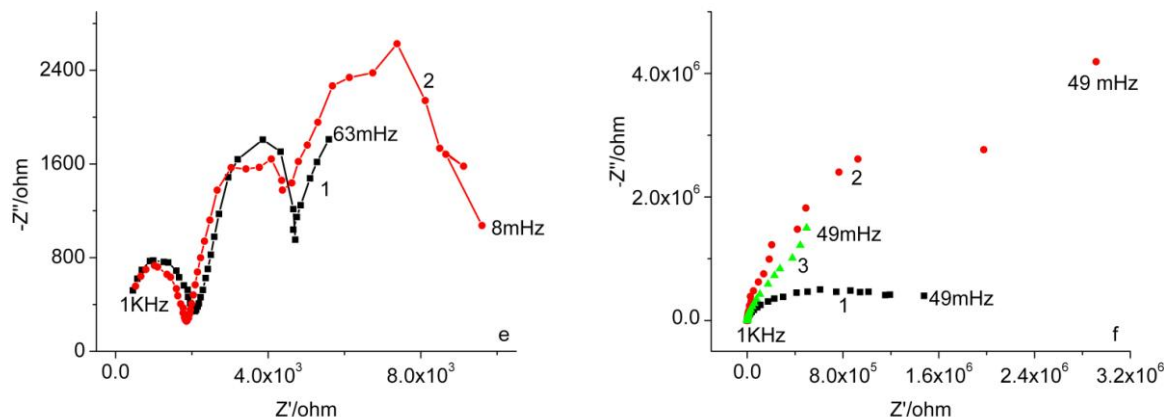
Figure 8. Nyquist plots for 0.19 M histidine-0.095 M sodium molybdate at pH 8.5, 1000 Hz to 5 mHz; a) 1) -0.1 V, 2) -0.05 V, 3) 0.0 V; b) 1) 0.03 V, 2) 0.05 V; 3) 0.07 V, 4) 0.08 V; c) 1000Hz – 5 mHz, 1)0.09 V, 2) 0.1 V, 3) 0.11 V; d) 1000 Hz to 82 mHz, 1) 0.12 V, 2) 0.13 V, 3) 0.14 V, 4) 0.15 V; e) 1) 0.2 V, 2) 0.3 V; f) 1) -0.8 V, 2) -0.6 V, 3) -0.25 V

On changing the potential from 0.11 to 0.12 V, the impedance loci observed in 4 quadrants suddenly changed into two capacitance curves and one inductive loop. At more positive potentials this two capacitance curves and one inductive loop became more symmetric at 0.15V. At still more positive potentials of 0.2V and 0.3 V, the inductive loop disappeared and three capacitance curves were observed. Thus at fairly anodic potentials, where passivation of mercury may interfere with the chemistry of the system, two or three adsorbed species became dominant.
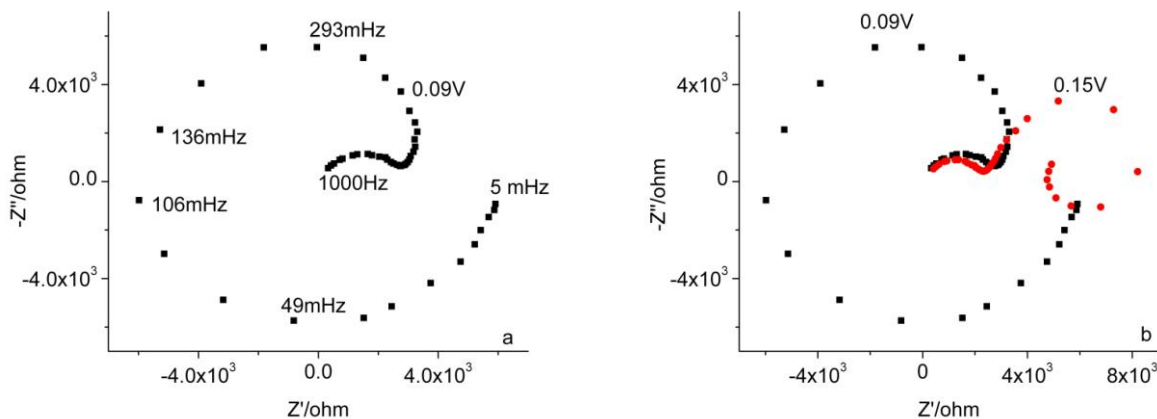
Figure 9. Nyquist plots exhibiting highly symmetric behavior for 0.19 M histidine-0.095 M sodium molybdate at a) 0.09 V and b) 0.09 V and 0.15 V

The symmetric nature of the impedance loci in four quadrants at 0.09 V and the capacitance curves and an inductive loop at 0.15 V for the 0.19 M histidine-0.095 M sodium molybdate mixture are shown in Figure 9.

3.3.3. Dependence of impedance on the concentration of 2 to1 histidine to molybdate

Nyquist plots for 0.019 M histidine-0.0095 M sodium molybdate, pH 7.9 and 0.038 M histidine-0.019 M sodium molybdate, pH 8.0 at different potentials are shown in Figures 10 and 11 respectively. The general features of these plots were the same except that with decreasing concentration there was a slight anodic shift in the potential at which negative differential resistance was observed. Also the impedance loci observed in the four quadrants were less symmetric. In all cases the double capacitance curves followed by induction were observed at 0.15 V. The comparative data at 0.09 V and at the optimum potentials for the three concentrations of histidine and ratio of histidine to molybdate of 2 to1 shown in Figure 12 have confirmed that the higher the concentration the more the cathodic shift in the potential for optimum impedance loci occurring in the four quadrants. Also the initial capacitance curve at the highest frequencies decreased with increasing concentration. These data suggest that spatial periodicities at the double layer that facilitate global coupling are better in the presence of molybdate and at higher concentrations.
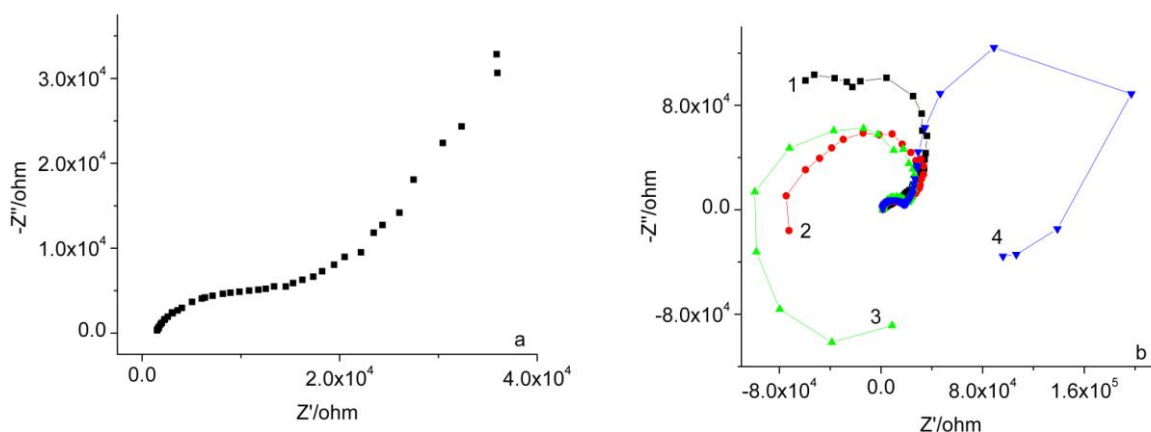
Figure 10. Nyquist plots for 0.019 M histidine-0.0095 M sodium molybdate, pH 7.9 a) 0.05 V; b) 1) 0.09 V, 2) 0.12 V, 3) 0.13 V, 4) 0.15V
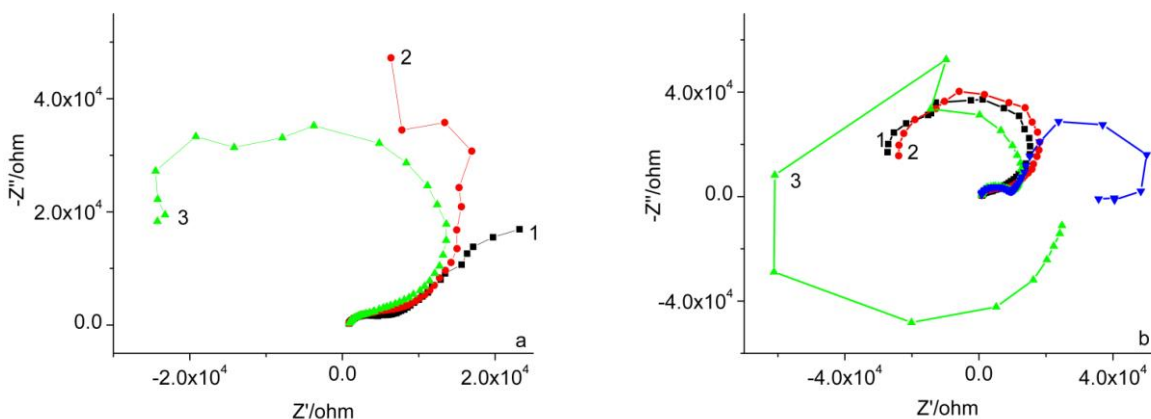
Figure 11. Nyquist plots for 0.038 M histidine-0.019 M sodium molybdate, pH 8.0 a) 1) 0.00 V, 2) 0.03 V, 3) 0.05 V; b) 1) 0.07 V, 2) 0.09 V, 3) 0.12 V, 4) 0.15V
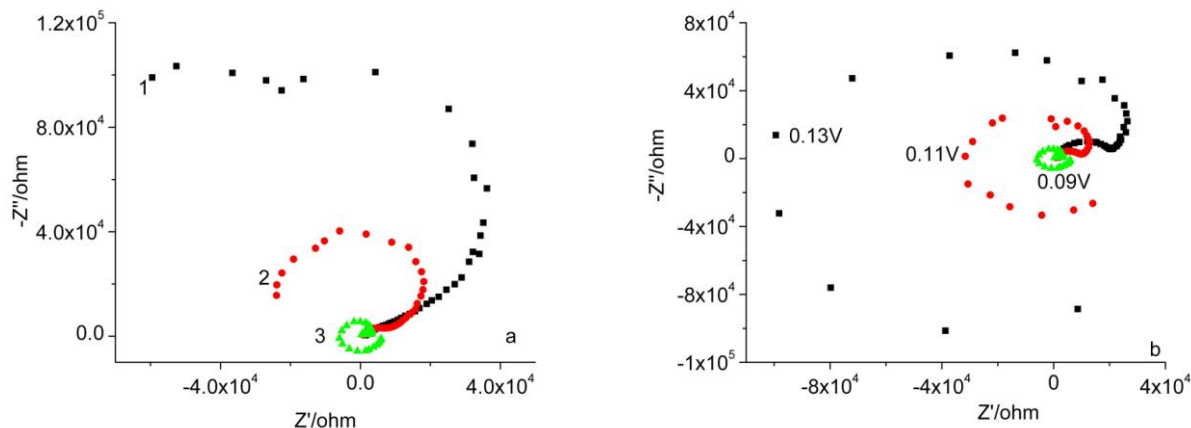
Figure 12. Nyquist plot at a) 0.09 V for 1) 0.019 M histidine-0.0095 M sodium molybdate; 2) 0.038 M histidine-0.019 M sodium molybdate; 3) 0.19 M histidine-0.095 M sodium molybdate; b) 0.13 V, 0.019 M histidine-0.0095 M sodium molybdate; 0.11 V, 0.038 M histidine-0.019 M sodium molybdate; 0.09 V, 0.19 M histidine–0.095 M sodium molybdate

3.3.4. Dependence of impedance on the ratio of histidine to molybdate

Our main reason for choosing the ratio of histidine to molybdate as 2 to1 was based on considerations of the protonated form of histidine and the divalent nature of molybdate. Of course we have not made exact calculations of the concentration of the protonated form at the experimental pH and therefore the chosen ratios are not optimum. The impedance results for 0.19 M histidine-0.095 M sodium molybdate and 0.19 M histidine-0.19 M sodium molybdate at three potentials are shown in Figure 13. These data suggested a preferred ratio of 1to1 for histidine and molybdate for obtaining impedance loci in four quadrants at potentials removed from the passivation region of mercury. With a histidine to molybdate ratio of 1to1 there was a10-20 mV cathodic shift in impedance loci occurring in four quadrants. However the data were not very compelling.
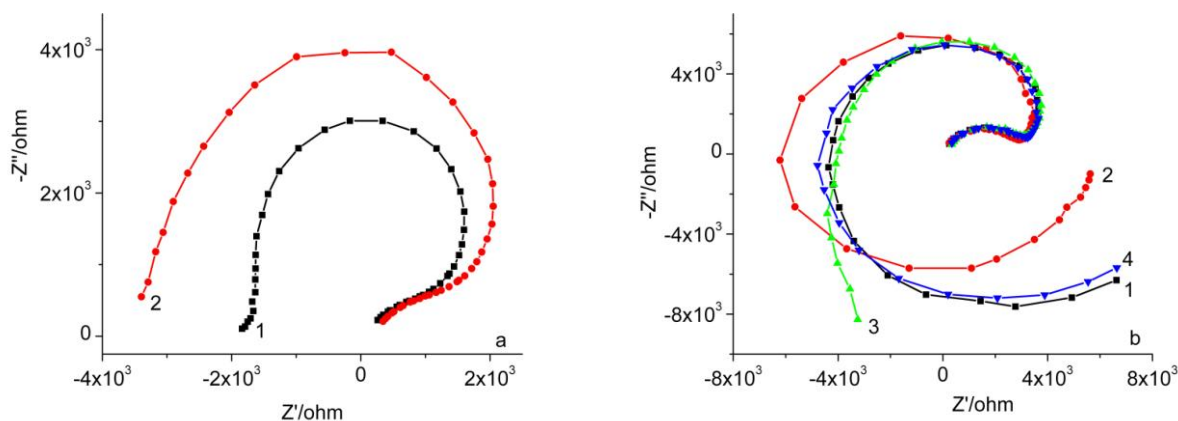
Figure 13. Nyquist plot at 0.0 V for a) 1, 0.19 M histidine and 0.19 M sodium molybdate; 2, 0.19 M histidine and 0.095 M sodium molybdate; b) 1, 0.07 V; 2, 0.08 V for 0.19 M histidine and 0.19 M sodium molybdate; 3, 0.07 V; 4, 0.08 V for 0.19 M histidine and 0.095 M sodium molybdate

3.3.5. Influence of pH on the impedance of 1to1 histidine to molybdate

The pH of 0.19 M histidine-0.19 M sodium molybdate mixture was slightly changed by adding small amounts of either NaOH or HCl. This was expected to change the ratio of protonated to nonprotonated histidine and consequent interactions with molybdate. These slight pH changes were not expected to change the nature of the aqueous molybdate. We did not want the pH to deviate too much from the biological pH.

The impedance data after adding a small amount HCl to 0.19 M histidine-0.19 M sodium molybdate are given in Figure 14. At -0.1 V a small capacitive behavior was observed. This capacitance increased at 0.0 and 0.03 V. Impedance loci in 4 quadrants were observed starting at 0.06 V. This became more and more optimum until 0.15 V (curves 1-6 in Figure 14). At 0.17 V, there were still impedance loci in the four quadrants but the impedance was much higher than at 0.15 V. With further increase in potentials to 0.18 V, the impedance exhibited two capacitance curves and an inductance. At 0.20 V, this two capacitive and one inductive behavior became more symmetric as shown in Figures 14c and 14d.
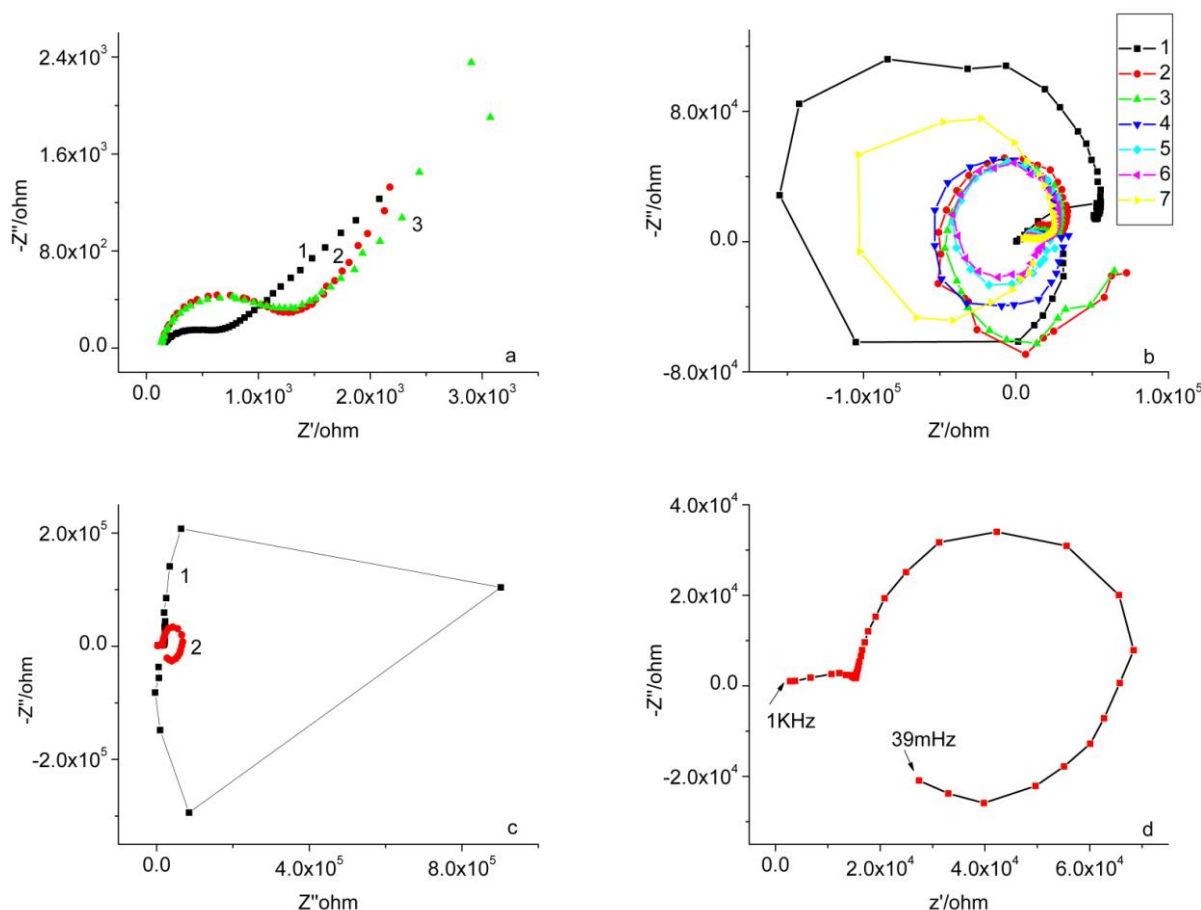
Figure 14. Voltage dependence of impedance of 0.18 M L-histidine- 0.18 M sodium molybdate, 0.067 M HCl, pH 7.5, a) 1) -0.1 V, 2) 0.00 V, 3) 0.03 V; b) 1) 0.06 V, 2) 0.07 V, 3) 0.08 V, 4) 0.11 V, 5) 0.13 V, 6) 0.15 V, 7) 0.17 V; c) 1) 0.18 V, 2) 0.20V; d) 0.20 V repeated from Figure 14 c
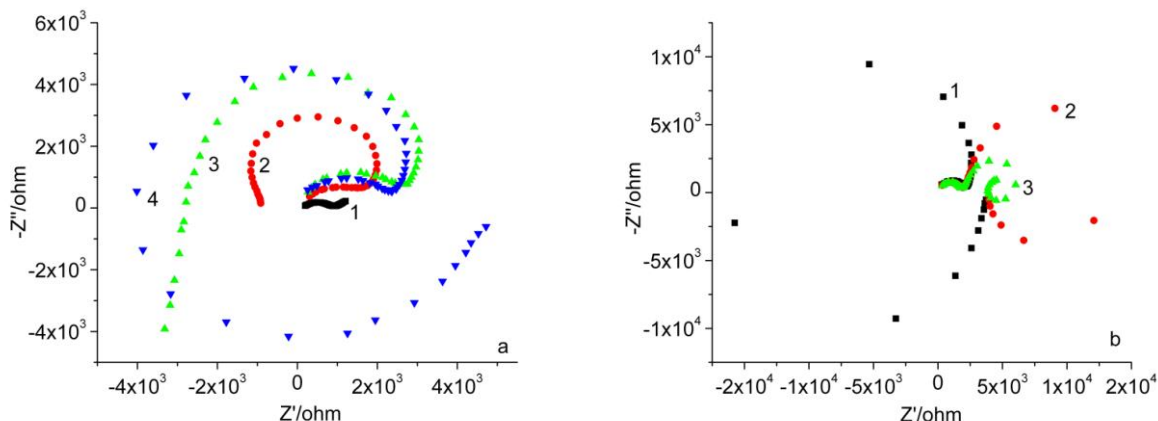
Figure 15. Voltage dependence of impedance of 0.18 M L-histidine- 0.1 M sodium molybdate, 0.067 M NaOH, pH 9.6, a) 1) -0.1 V, 2) 0.00 V, 3) 0.03 V, 4) 0.05 V; b) 1) 0.07 V, 2) 0.09 VV, 3) 0.11 V [24]

The impedance data after adding a small amount of NaOH to 0.19 M histidine-0.19 M sodium molybdate are given in Figure 15. The general features are similar to that at pH 7.5. However at pH 7.5 the initial capacitance curve at higher frequencies decreased with increasing anodic potentials. On the other hand at pH 9.6 the initial capacitance curve increased with increasing anodic potentials. Also there was no negative differential resistance observed even at 0.03 V at pH 7.5 whereas there was NDR at 0.0 V for pH 9.6. In other words there was a slight cathodic shift in potential for observation of NDR with increasing pH.

A comparison of the impedance data at two different potentials, 0.0 V and 0.07 V for pH 7.5, 8.5 and 9.6 shown in Figure 16 has further validated the above results.
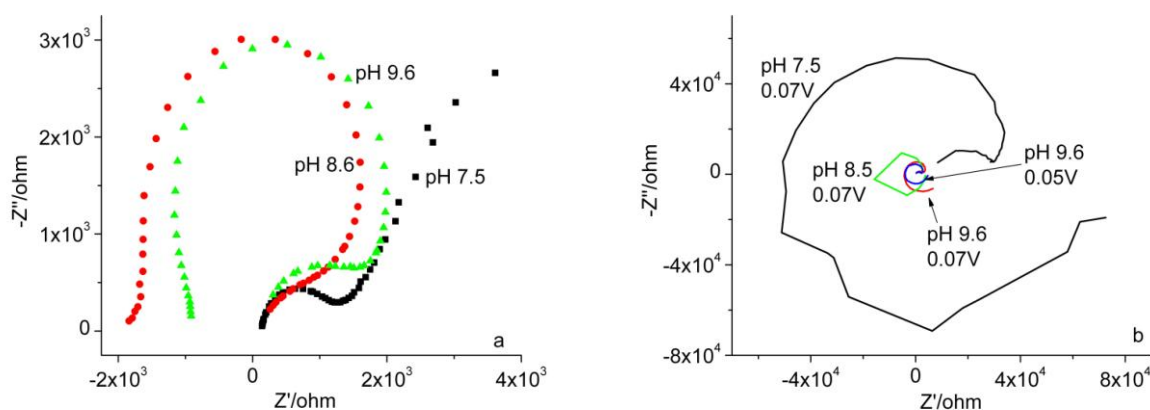
Figure 16. Comparison of pH dependence of impedance at a) 0.0 V; b) 0.07 V; pH 7.5 solution has 0.18 M histidine-0.18 M sodium molybdate, 0.067 M HCl; pH 8.5 solution has 0.19 M histidine-0.19 M sodium molybdate; pH 9.6 solution has 0.18 M histidine-0.18 M sodium molybdate, 0.067 M NaOH

For comparing the influence of potentials, concentrations, and pH one has to make a wide variety of choices because for each concentration or pH the optimum potential at which the impedance

loci occurred in 4 quadrants were slightly different. Figure 16b also includes the data at 0.05 V for pH 9.6 solution. These results have also demonstrated another fact that passivation of mercury at these slightly anodic potentials have in no way affected the general conclusions. Moreover we have observed such complex impedance behavior at cathodic potentials for mercury [24, 25].

3.4. Stability

The Nyquist plots for a set of four experiments with 0.19 M L-histidine - 0.095 M sodium molybdate, at pH 8.5, at 0.09V and in the frequency range 1000 Hz to 5 mHz are shown in Figure 18. Considering the complicated nature of the impedance curve, the data are quite reproducible with practically no scatter.
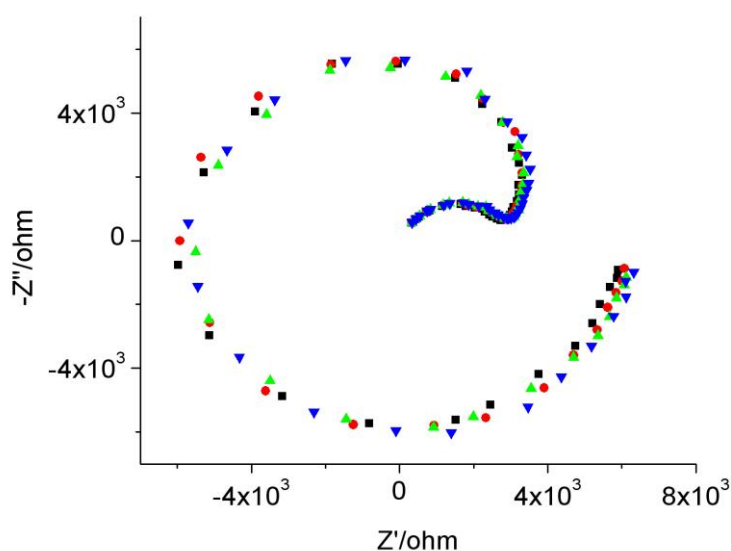
Figure 17. Impedance of 0.19 M L-histidine- 0.095 M sodium molybdate, pH 8.5, 0.09V, 4 sets of data

We had mentioned earlier that one could manipulate the visual observation of less scatter by choosing Bode plots to show reproducibility [26].

3.5. Surface Area

Surface inhomogeneities make the use of solid electrodes extremely difficult to investigate the influence of surface area on the phenomenon of spatiotemporal periodicities. In this respect, use of liquid mercury as working electrode offers a great advantage in providing fresh surface as well as desired area each time. In the PAR 303A SMDE tri-electrode system, there are small, medium, and large size drop controls. The surface area of the working electrode was varied by controlling the drop

size of the mercury by pushing the dispense button for the appropriate number of times before the mercury falls.
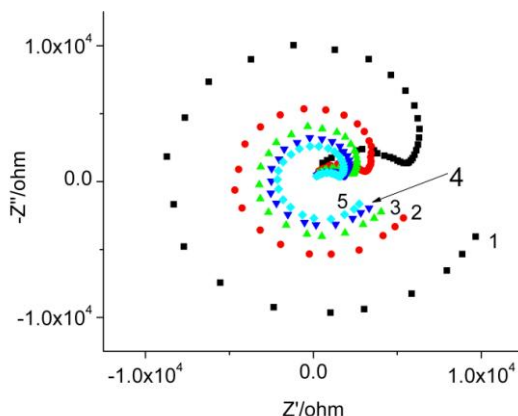
Figure 18. Nyquist plot for 0.177 M L-histidine- 0.177 M sodium molybdate, 0.067 M NaOH, pH 9.60, 0.05V, influence of surface area of mercury drop, mm^2 1) 0.011, 2) 0.017, 3) 0.022, 4) 0.027, 5) 031 [24]

The Nyquist plots for 0.177 M L-histidine - 0.177 M sodium molybdate, 0.067 M NaOH, at pH 9.6 and at 0.05V are given in Figure 19. Highly symmetric and smooth impedance spectra exhibiting loci in four quadrants are obtained in all cases. With increasing surface area the impedance also became less and less in all the four quadrants. We have reason to believe, as in the case of palladium-lipoate complex, that with increase in surface area, the possibility of self-assembled layers of histidine-molybdate near the double layer increased with increased possibility of long range electron transfer [4]. In biological enzyme systems such as molybdoenzyme nitrate reductases, NDR is attributed to diode-like behavior [27].

The impedance loci observed in the first two quadrants, with characteristic negative differential resistance (NDR), has been attributed to the transition from the nonminimum phase-type to the minimum phase-type and corresponded to the Hopf bifurcation under current control [7]. Also the resonance-like maximum of the amplitude characteristic or impedance modulus was indicative of harmonic relaxation along with the phase change behavior for the first order (discontinuous) nonminimum phase to the second order (continuous) minimum phase [7]. Insights into the instabilities or bifurcations and distinction between saddle-node and Hopf bifurcations are often obtained from impedance spectroscopy [7, 9, 28-33]. In living systems, non-stationary regimes far from equilibrium are very prevalent and many of these systems exhibit bifurcations and spatiotemporal periodicities. From our examples of cysteine-molybdate, lysine-molybdate, and currently histidine-molybdate, we are tempted to conclude that molybdate provides a pathway for long range signaling. Cysteine and histidine, in the absence of molybdate, produced some impedance oscillations at these potentials instead of multi-quadrant impedance. While adsorption may play a significant role in the observed multiquadrant impedance behavior, it is certainly not due to the passivation of mercury. The electronic character of the global coupling is evident because of the specificity of the observed impedance

behavior to a narrow range of potentials and the smooth change in impedance loci passing from one, to two, to three, and four quadrants initially and then changing the trend in impedance with one, two, or three capacitance curves and inductance. Also the multi-quadrant impedance behavior is not observed with histidine only. We suggest that the one electron reduction product of 2-oxo histidine, a free radical, is involved in providing the electronic character to the self assembled layers of histidine-molybdate at or near the double layer. Mercury working electrode has provided a great advantage for repetition of the experiments because a fresh drop can be easily obtained each time with controlled surface area and minimum surface inhomogeneities. Our main aim was to investigate numerous biological systems with characteristic NDR rather than to delve deeply into the bifurcation phenomena.

4. CONCLUSIONS

We have investigated the cyclic voltammetric behaviour of L-histidine in the absence and presence of sodium molybdate. Since no electrolytes were used, the concentration of the histidine used was fairly high. The results revealed that molybdate enhanced the oxidation of histidine. Reduction of the presumed oxidation product of histidine, 2-oxohistidine, produced cathodic current oscillations. The cathodic and anodic currents and the cathodic current oscillations were much higher in the presence of molybdate. A comparison of the cyclic voltammograms also revealed strong interactions of molybdate with histidine and also the presence of molybdate in the oxidized histidine. The U-V absorption spectra indicated specific interaction between histidine and molybdate. Impedance exhibited negative differential resistance and impedance loci in all four quadrants depending on the applied potential. In the absence of molybdate, somewhat chaotic impedance oscillations instead of NDR were observed. When the concentrations of histidine-molybdate were increased, the four quadrants impedance spectra became more symmetric. When the ratio of histidine to molybdate was changed from 2: 1 to 1:1, the NDR observed was better. With increase in pH, a slight cathodic shift was observed in the potential at which NDR was observed. At lower pH, the four quadrants impedance spectra were observed in a wider range of potentials of about 100 mV. At more anodic potentials after the four quadrants impedance spectra, the nature of impedance changed to double capacitance and an inductive loop and then finally to three capacitance curves. In the presence of molybdate, the data suggested that self-assembled layers of histidine-molybdate near the double layer increased the possibility of long range electron transfer, and are in many ways similar to the electronic behavior exhibited by enzymes. The one electron reduction product of 2-oxohistidine, a free radical, is believed to be responsible for this observed NDR.

References

1. D. Voet and J.G. Voet, *Biochemistry*, 2nd edition, John Wiley & Sons, Inc, New York (1995)
2. N. Bagheri, *J. Phys. Chem. and Electrochem.*, 1 (2010) 1
3. R. J. Field and L. Gyorgyi, Editors in *Chaos in Chemistry and Biochemistry*, World Scientific Publishing Co., NJ 07661, USA (1993)
4. C. V. Krishnan and M. Garnett, *Liquid crystal behavior in solutions, electrode passivation, and impedance loci in four quadrants,* P. Marcus and V. Maurice Editors *in Passivation of Metals and Semiconductors, and Properties of Thin Oxide Layers*, Elsevier, New York (2006) 389
5. M.T.M. Koper, *Adv. Chem. Phys.*, 92 (1966) 161
6. S. Fukushima, S. Nakanishi, K. Fukami, S. Sakai, T. Nagai, T. Tada, and Y. Nakato, *Electrochem.Commun.*, 7 (2005) 411
7. A. Sadkowski, M. Dolata, and J. P. Diard, *J. Electrochem. Soc.*, 151(2004) E-20
8. K. Krischer in B. E. Conway, J. O'M. Bockris, and R. E. White (Editors), in *Modern Aspects of Electrochemistry*, No. 32, Plenum Publishers, New York, Chapter 1 (1999) 1
9. P. Strasser, *The Electrochemical Society Interface*, Winter (2000) 46
10. C.V. Krishnan, M. Garnett, and B. Chu, *Int. J. Electrochem. Sci.,* 3 (2008) 854
11. C.V. Krishnan, M. Garnett, and B. Chu, *Int. J. Electrochem. Sci.,* 3 (2008) 873
12. C. V. Krishnan, *Int. J. Electrochem. Sci.,* 8 (2013) ---
13. A. Marina, C. D. Waldburger, and W. A. Hendrickson, *The EMBO Journal,* 24 (2005) 4247
14. K. Uchida and S. Kawakishi, *J. Biol. Chem.*, 269 (1994) 2405
15. E. K. Hodgson and I. Fridovich, *Biochem.*, 14 (1975) 5294
16. R. L. Levine, C. N. Oliver, R. M. Fulks, and E. R. Stadtman, *Proc. Natl. Acad. Sci. U. S. A.,*78 (1981) 2120
17. R. Z. Cheng, K. Uchida, and S. Kawakishi, *Biochem. J.*, 285 (1992) 667
18. F. Zhao, E. G. Schöneich, G. I. Aced, J. Hong, T. Milby, and C. Schöneich, *J. Biol. Chem.*, 272 (1997) 9019
19. L. C. Chen, C. C. Chang, and H. C. Chang, *Electrochim. Acta*, 53 (2008) 2883
20. K. Ogura, M. Kobayashi, M. Nakayama, and Y. Miho, *J. Electroanal. Chem.*, 463 (1999) 218
21. V. Brabec and V. Mornstein, *Biophys. Chem.*, 12(2) (1980) 159
22. B. Malfoy and J. A. Reynaud, *J. Electroanal. Chem. and Interfacial Electrochem.*, 114 (1980) 213
23. Y. C. Weng and T. H. Cheng, *Z. Naturforsch.*, 66b (2011) 279
24. C. V. Krishnan, M. Garnett, and F. Antonawich, *Mitochondrial Dysfunction and Cancer:Modulation by Palladium α-Lipoic Acid Complex, in Advances in Nanoscience and Nanotechnology*, Volume 2 "*Nanomedicine and Cancer Therapies*", S. Thomas, M. Sebastian, A. George, and Y. Weimin, Series Editors and M. Sebastian, N. Ninan, and E. Elias, Volume Editors, Apple Academic Press, and CRC Press (Taylor and Francis Group), Chapter 7 (2013) 75
25. C.V. Krishnan, M. Garnett, and B. Chu, *Int. J. Electrochem. Sci.*, 3 (2008) 1364
26. C. V. Krishnan and M. Garnett, *Electrochim. Acta*, 51 (2006) 1541
27. A. Sucheta, B. A. C. Ackrell, B. Cochran, and F. A. Armstrong, *Nature*, 356 (1992) 361
28. M. T. M. Koper, *J. Chem. Soc. Faraday Trans.*, 94 (1998) 1369
29. M. Keddam, H. Takenouti, and N. Yu, *J. Electrochem. Soc.*, 132 (1985) 2561
30. D. D. Macdonald, *Electrochim. Acta*, 35 (1990) 1509
31. B. A. Boukamp, *J. Electrochem. Soc.*, 142 (1995) 1885
32. Y. Mukouyama, S. Nakanishi, T. Chiba, K. Murakoshi, and Y. Nakato, *J. Phys. Chem.*, 105 (2001) 7246
33. C.V. Krishnan, M. Garnett, and B. Chu, *Int. J. Electrochem. Sci.*, 2 (2007) 444